MECHANOCHEMISTRY AND MECHANICAL ALLOYING 2003

JOURNAL OF MATERIALS SCIENCE **39** (2004) 5201 – 5207

Phase formation study of PZT nanopowder by mechanical activation method at various conditions

A. BEITOLLAHI*, M. MORAVEJ
Ceramic Division, Department of Metallurgy and Materials Engineering, Iran University of Science and Technology, Narmak, Tehran, Iran
E-mail: beitolla@iust.ac.ir

In this work, attempt is made to prepare and study the phase evolution of nanocrystalline $Pb(Zr_{0.53}Ti_{0.47})O_3$ powder with both planetary and high energy shaker mill in air atmosphere, using X-ray diffraction (XRD) and transmission electron microscopy (TEM). Three different series of samples with various processing conditions i.e., ball to powder weight ratio (BPR) of 10/1. 20/1 at 500 rpm and 10/1 ratio at 250 rpm, were prepared using a planetary mill. Further, another series of samples were also prepared using a high energy shaker mill with BPR = 10 at 900 rpm. The BPR was seen to have a marked effect on the phase formation of PZT nanocrystalline powder. While the formation of some nanocrystalline intermediate phases of wide compositional distribution in an amorphous matrix was confirmed for the samples prepared using planetary mill with BPR = 10 at 250 and 500 rpm, single phase PZT could be formed when prepared at BPR = 20 at 500 rpm. Further, it was also shown that the formation of single phase PZT nanocrystalline powder of an average crystallite size of 10 nm could take place after only 30 h of milling when activated by shaker mill with BPR = 10 at 900 rpm. The results obtained are related to the rate of the injected energy and diffusion processes taken place. *© 2004 Kluwer Academic Publishers*

1. Introduction

Nanostructured materials (NSM) have received wide attention during the last decade because of their interesting and novel properties [1–3]. Amongst various preparation routes, mechanical alloying (MA) by high-energy milling is an easy and inexpensive route for producing NSM in bulk quantities with excellent scope of microstructural and process control. This technique have been also recently used to synthesize various nanosized magnetic and ferroelectric ceramic powders such as; Fe_2O_3 [4], ZrO_2 [5], $MnZnFe_2O_4$ [6], $Pb(Zn_{1/3}Nb_{2/3})O_3$-$BaTiO_3$ [7], $BaTiO_3$ [8], $Pb(Zr_{0.53}Ti_{0.47})O_3$ (PZT) [9], $PbTiO_3$ [10]. Lead Zirconate Titanate $PbZr_{1-x}Ti_xO_3$ (PZT) ceramics are well known for their very important and interesting dielectric, electro-optic and piezoelectric properties [11]. The preparation of this compound is normally based on conventional ceramic route or various chemical routes [12–14]. However, mechanical activation lends itself very advantageous for the synthesis of this compound since there is no need of heat treatment and expensive raw materials [15]. Of course, measures should be taken regarding the introduction of impurities during milling process. This preparation route although practically very simple but is a complex process which depends on many factors, for instance on physical and chemical parameters such as the precise dynamic conditions, temperature, nature of the grinding tools [16, 17]. For most of the compounds prepared by this technique various processing conditions such as ball to powder weight ratio (BPR), milling speed and milling type have shown [18] to have significant effect on the final product formed. Therefore, in the work presented here, attempt is made to study the phase formation of $Pb(Zr_{0.53}Ti_{0.47})O_3$ compound at various processing conditions such as; BPR, milling speed and milling type.

2. Experimentals

The PZT composition selected for this study was $Pb(Zr_{0.53}Ti_{0.47})O_3$, which is near the morphotropic phase boundary in PZT's phase diagram. The starting materials were PbO (>99% purity, Merck, Germany), ZrO_2 (>99% purity, Tosoho, Japan) and TiO_2 (>99% purity, Merck, Germany). Appropriate amounts of the constituent oxides, as required for the stoichiometric PZT composition, were mixed together in ethanol using zirconia balls of 10 mm in diameter as the milling media and a cylindrical polyethylene jar in a laboratory ball mill for 70 h. The obtained slurry dried in an oven at 80°C for 3 h and the dried powder lumps was ground

---

*Author to whom all correspondence should be addressed.

using an agate mortar and pestle. This was then passed through a 200 mesh sieve. Mechanical activation of the powder mixture was carried out using two different mills; a planetary mill and a Spex 8000 shaker mill. For the milling process using planetary mill a cylindrical tungsten carbide vial 40 mm in diameter and 40 mm in length with four tungsten carbide balls 10 mm in diameter were used. Two different milling speeds and ball to powder weight ratios (BPR) were selected. The first milling process by planetary mill was set at about 250 rpm with BPR = 10 for 100 h. The samples were collected at 20, 30, 50, 60, 100 h. For the other two series of samples, the milling speed was set at about 500 rpm and two process with BPR = 10 and BPR = 20 were carried out. The milling times were 120 h for BPR = 10 and 75 h for BPR = 20. The samples were collected at 10, 20, 50, 80, 120 h for BPR = 10 and 5, 20, 70 h for BPR = 20. The sample collected after 20 h of milling with 500 rpm and BPR = 20 was calcined at 500, 600, 650 and 800°C for 2 h to study the effect of mechanical activation on the formation temperature of PZT. A cylindrical stainless steel vial 50 mm in diameter and 70 mm in length and four stainless steel balls 10 mm in diameter and BPR = 10 were used for the milling process with Spex 8000 shaker mill at about 900 rpm. The milling time was set for 50 h and the samples were collected at 10, 20, 30, 40, 50 h. Phase development in the samples was monitored using a Philips X-ray diffractometer (XRD) with Cu $K_{\alpha 1}$ radiation. A 200-KV Transmission electron microscopy (TEM) was used to study the changes in the powder morphology and crystallinity of the milled samples collected after 10, 50, 120 h milling by planetary mill at 500 rpm and BPR = 10.

3. Results and discussion

Fig. 1 display XRD multiplot of PZT powders picked up at various time intervals, prepared by planetary mill with a BPR of 10/1 at 250 rpm. As expected prior to mechanical activation, the powder mixture exhibited sharp peaks of crystalline PbO, ZrO_2 and TiO_2, as no or little reaction was triggered by the conventional ball milling. However, upon 20 h of mechanical activation, almost all the sharp peaks of mixed oxides have vanished. The significant broadening in diffraction peaks upon 20 h of mechanical activation suggests that a significant refinement in crystallite and particle sizes of the constituent oxides together with a degree of amorphization have been initiated by the mechanical activation. It should be mentioned that, by increasing the milling time, particle size reduction is mainly replaced by increasing dislocation and defects concentration. The development of large number of dislocations, and their associated strain fields, may lead to an overall decrease in long-range lattice periodicity, normally evidenced by line broadening and disappearance of diffraction peaks on X-ray diffraction (XRD) patterns or the appearance of halo diffraction peaks in TEM micrographs. In addition, or alternatively, the increase in internal energy may promote transition to less thermodynamically stable crystalline phases in compounds that exhibit polymorphism. The energy of any stress field formed can change into heat which, in turn initiate chemical reactions and lead to the annealing of some defects. Increasing the milling time, however, for these series of samples (Fig. 1) caused further rise of the background of diffraction peaks. This suggests that the fraction of amorphous phase has possibly increased by milling time for these series of samples. As seen from Fig. 1, XRD measurements of the picked up powder samples after 20, 30 and 60 h did only

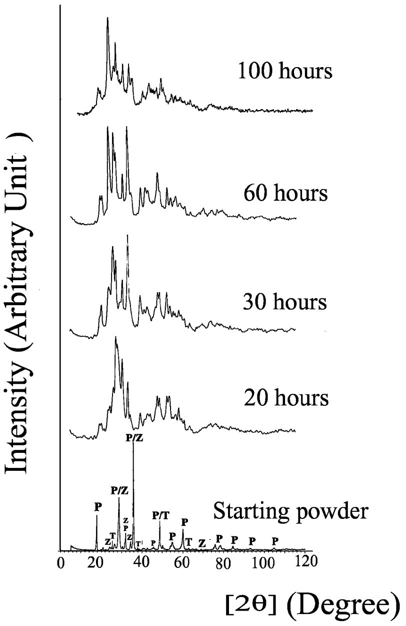

Figure 1 XRD patterns of the powder mixture subjected to mechanical activation for various time intervals using a planetary mill with BPR = 10 at 250 rpm. (P) PbO, (Z) ZrO_2, (T) TiO_2.

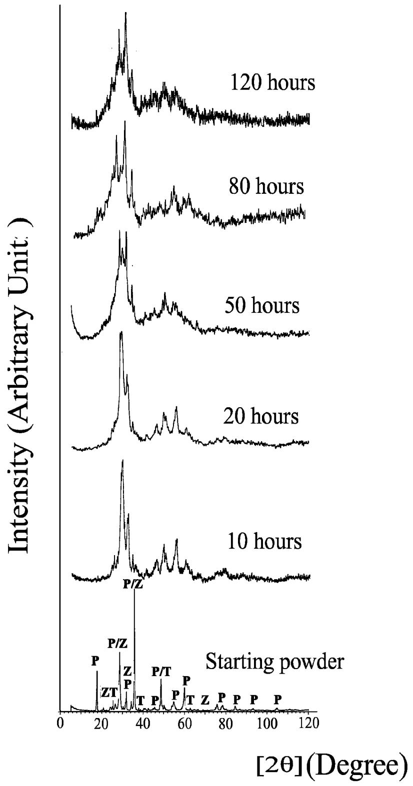

Figure 2 XRD multiplot of the samples subjected to mechanical activation for various time intervals using a planetary mill with BPR = 10 at 500 rpm. (P) PbO, (Z) ZrO_2, (T) TiO_2.

confirmed the formation of some complex unknown intermediate solid solutions with d spacing values very close to PbO and ZrO_2 (presented as $(PbO)_{ss}$ and $(ZrO_2)_{ss}$) as well as an amorphous phase.

Increasing the milling time to as high as 100 h did not eventually give rise to the formation of single phase PZT (Fig. 1). Kong *et al.* [19] have shown that for the PZT samples prepared by planetary milling at 200 rpm and a BPR of 20/1 the onset of formation of PZT phase starts only after about 20 h of milling and further increase of the milling time to as high as 60 h gave rise to the formation of single phase nanocrystalline PZT. This implies that the lower BPR i.e., 10/1 applied for these series of samples prepared in this work have possibly had a marked influence on the phase evolution of these series of samples. Fig. 2 shows the XRD multiplot obtained for samples picked up at various time intervals, e.g., 0, 10, 20, 50, 80 and 120 h prepared by planetary mill with a BPR of 10/1 at 500 rpm. Again, as is evident from this figure, for these series of samples, almost all the sharp peaks of mixed oxides have vanished after 20 h of mechanical activation. Further, as can be understood from this multiplot, increasing the milling time to as high as 120 h did not also cause the formation of single phase PZT. Instead, increasing the milling time was seen to increase the fraction of amorphous phase (Fig. 2). Fig. 3 shows TEM micrograph of the sample milled for 120 h as well as EDX-spectrum of powder particles. The Ni-peak appeared in the EDX spectrum stems from the supporting grid. This figure suggests a highly agglomerated state for the powder obtained. Further, EDX-spectra obtained from different sites of powder particles milled for 10 h revealed the existence of quite different compositions confirming the results obtained by XRD for this series of samples. TEM examinations of the milled samples for 10 h, for these series of samples, showed complicated diffraction patterns due to the coexistence of many different phases with no evidence of amorphization. However, as Fig. 4 shows, after 50 h of milling diffuse halos appeared in the diffraction patterns obtained indicating the presence of an amorphous phase and after 120 h of milling again sharp diffraction rings and spots appeared (Fig. 5), indicating the presence of some crystalline phases. The observed d-spacings could be attributed to trigonal and rhombohedral PZT phases of various stoichiometry. The TEM results obtained for these series of samples confirmed that in the early stage of

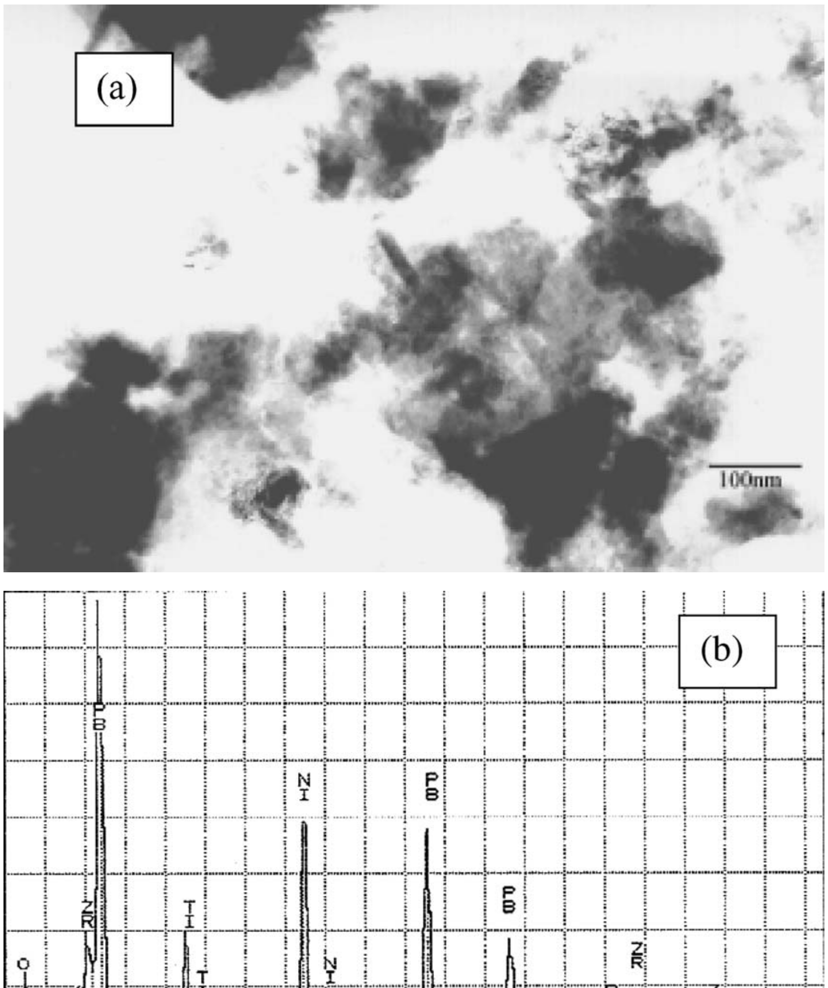

Figure 3 TEM micrograph of the sample prepared by milling (BPR = 10, 500 rpm) (a) as well as EDX spectra obtained (b). The Ni-peak stems from the supporting grid.

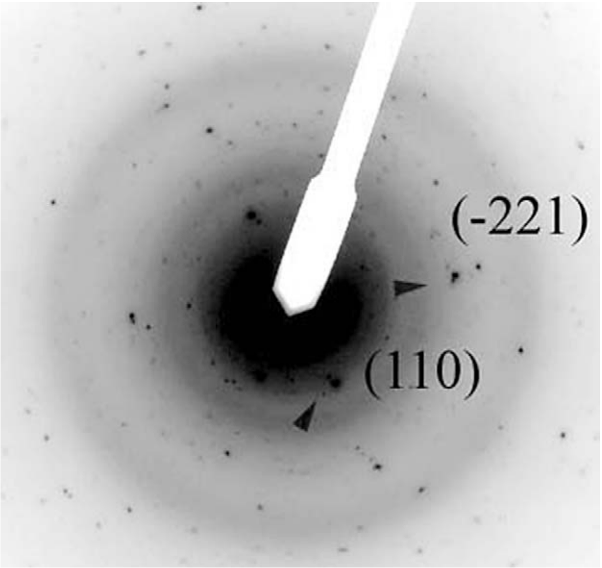

Figure 4 TEM diffraction pattern for the sample prepared using a planetary mill with BPR = 10 at 500 rpm after 50 h of milling.

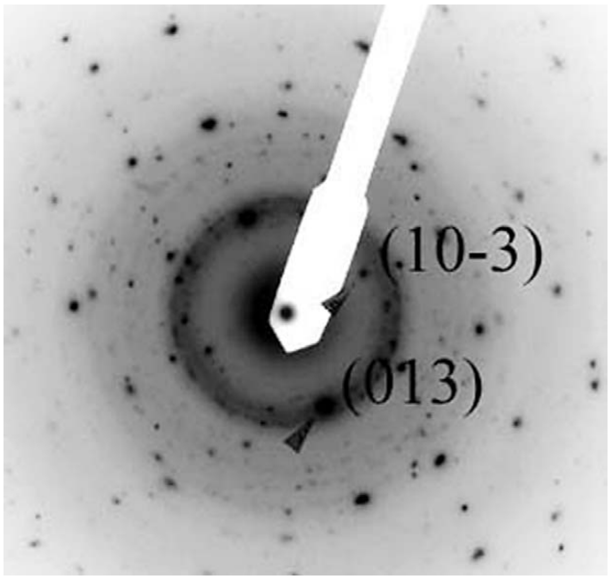

Figure 5 TEM diffraction pattern for the sample prepared using a planetary mill with BPR = 10 at 500 rpm after 120 h of milling.

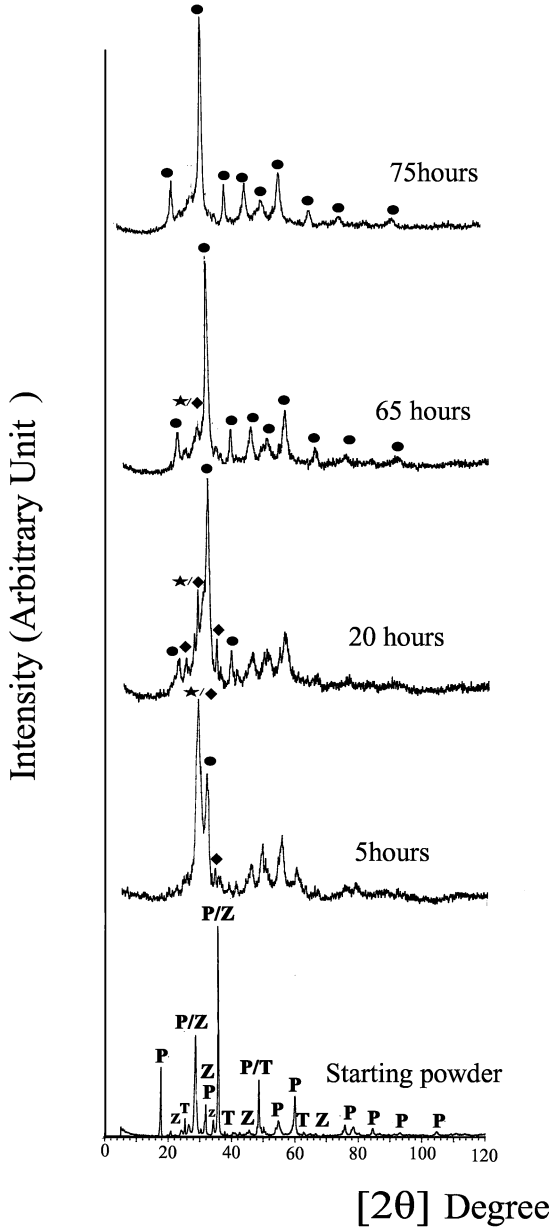

Figure 6 XRD patterns of the powder mixture subjected to mechanical activation for various time intervals (BPR = 20, 500 rpm). In this figure (P) stands for PbO, (Z) for ZrO_2, (T) for TiO_2, (*) for $(PbO)_x$, (♦) for $(ZrO_2)_x$, (●) for PZT.

milling, particle size reduction and solid-state reaction proceeds. By further milling to up to 50 h of milling, formation of amorphous phase also takes place. Further, increasing of the milling time gave rise to the formation of some nanocrystalline phases in an amorphous matrix. However, as XRD multiplot obtained for these series of samples (Fig. 2) showed, the final product prepared after 120 h of milling did not solely composed of single phase nanocrystalline PZT phase. Fig. 6 displays the XRD multiplot obtained for non-activated and activated samples picked up at different time intervals e.g., 0, 5, 20, 65 and 75 h prepared by planetary mill with a BPR of 20/1 at 500 rpm. For the sample mechanically activated for 5 h, the sharp peaks of mixed oxides seen for non-activated sample have vanished which again suggests a significant refinement in crystalline and particle sizes of the constituent oxides as well as the formation of some intermediate solid solution phases. Further increasing the milling time for this series of samples (Fig. 6) gave rise to the formation of sharper peaks. After only 20 h of milling, for these series of samples, the formation of PZT phase was initiated as well as some intermediate solid solution phases possibly comprising of initial raw materials. Finally, after 65 h of milling the formation of single phase PZT was seen. The average crystallite size for the PZT phase formed estimated from XRD data [20] was ~10 nm. Comparing the back ground of the XRD patterns presented in Figs 1, 2 and 6, one can realize that the degree of amorphization is possibly lower when BPR and milling speed was higher. Further, TEM examinations for the 4 different sets of the samples prepared with different milling conditions are currently underway.

The formation of structural defects and disorder induced by mechanical activation will favor diffusion and atomic rearrangements at considerably low temperatures. The reaction rates are influenced by the initial contact area and diffusion of the reactant species through the product phases [21]. For most solid-state processes, the initial contact area is fixed and diffusion rate is limited. Therefore, solid-state reactions are essentially temperature dependent. This is not the case for the reactions induced by mechanical activation, since diffusion is a dynamic process. Further, a reaction can actually increase with increase in mechanical activation duration and change of phases [22, 23]. Considering that diffusion process during mechanical activation is a dynamic process one can assume that the interdiffusion layer is broken by the activation process, thus enabling new surfaces with very different compositions to contact each other. Therefore, repeated fracturing and re-binding enlarge the diffusion area, resulting in the enhancement of the diffusion kinetics. Mechanical activation minimizes the effect of product barriers on the reaction kinetics and provides the condition required for the promulgation of solid-state reactions at low temperature.

Further, diffusivity can be raised dramatically by reducing the grain size and increasing the temperature. The increase in diffusivity is physically due to a decrease in the grain size and the creation of more free surfaces, since both grain boundary and surface diffusions have much lower activation energies in comparison with lattice diffusion. The surface tends to be a region of relatively high disorder and therefore the activation energy for diffusion tends to be low. The activation energy in grain boundary is generally higher in comparison to that of surface diffusion. Whilst that for lattice diffusion is the highest value. As a result, at low temperatures, surface diffusion dominates over grain boundaries and lattice diffusions. As the temperature increases, grain boundary diffusion becomes more significant and at higher temperature, lattice diffusion becomes the principal mode for diffusion [24]. It should be added that the change from one predominant mechanism to another depends upon the nature of the grain boundaries and the surfaces, of course.

As shown, the formation of single phase PZT compound was not confirmed for the samples prepared by planetary mill with a BPR = 10 at 250 and 500 rpm. However, its formation was confirmed when the samples were subjected to a BPR = 20 at 500 rpm. Suggesting that the increase of the BPR have had a marked effect on the formation of PZT compound. The specific milling intensity is defined as the momentum transferred by the ball to the powder (BPR) involved in the collision per unit time.

It is expressed as:

$$I = \frac{M_\mathrm{b} V_\mathrm{max} f}{M_\mathrm{p}}, \tag{1}$$

where M_b is the ball mass, V_max the maximum velocity of the ball, f the ball shock frequency and M_p the mass of powder in the vial. Therefore it can be suggested that increasing the BPR through the decrease of the mass of the powder (M_p) have resulted in the increase of specific milling intensity. The ball shock velocity is related to the mill rotational speed and the impact frequency is related to the number of balls inserted into the vial. However, Abdellaoui and Gaffet [25, 26] showed that neither the shock energy nor the shock frequency governs the final product in a planetary ball mill if taken in

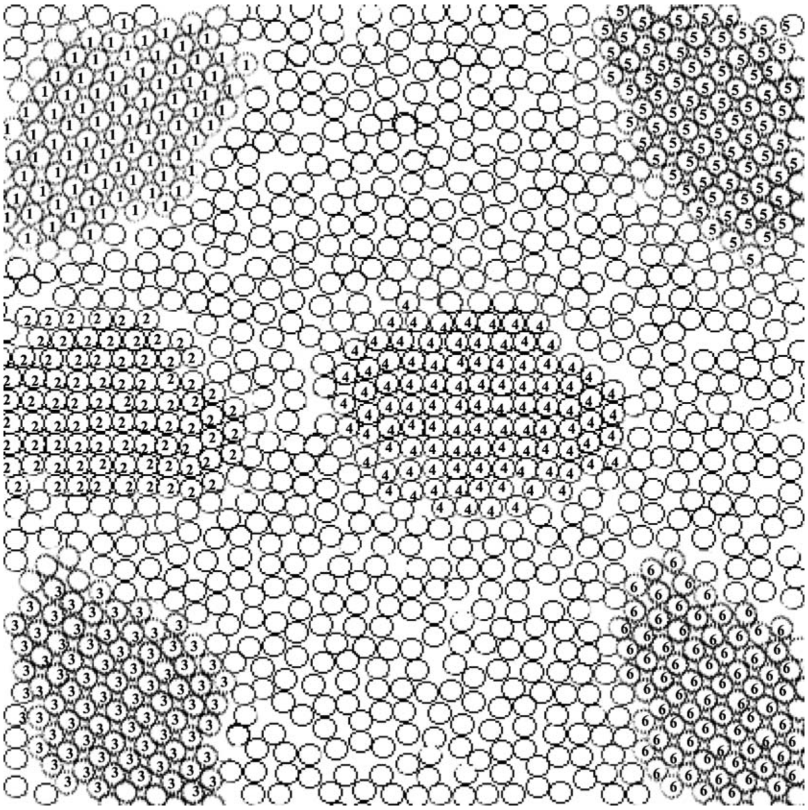

Figure 7 One dimensional representation of various nanocrystalline phases in an amorphous matrix. Various numbers given represents nanocrystalline areas of different compositions.

account separately, but only the injected shock power is responsible for the ball milled final product. The injected power is proportional to the product of shock frequency and shock energy. Further, Magini *et al.* [27] used an intensive factor in each collision event, ΔE, to express the energy transferred per unit quantity of material trapped in the collision event, as described in the following:

$$\frac{\Delta E}{Q_{\max}} = \left[7.66 \times 10^{-2} R_{\mathrm{p}}^{1.2} S^{0.6} E^{0.4}\right] d_{\mathrm{b}} \omega_{\mathrm{p}}^{-1.2} / \delta, \quad (2)$$

where $Q_{\max}$ is the maximum quantity of trapped material, R_{p} is the distance between center of disk and center of vial, S is the density of the milling balls, E is the Young Modulus, d_{b} is the diameter of the milling ball, ω_{p} is the angular velocity of vial and δ is the surface density of the covering powder. Further, they pointed out that the energy is not absorbed by the total powder but only by a small quantity of mass trapped in collision and the above equation (Equation 2) does not consider the influence of the ball number. Therefore, they suggested that considering the total collision frequency νt of the n_{b} balls and disconsidering the reciprocal hindering of balls, the powder which is involved in the milling process is given by the extensive factory:

$$P = \Delta E \cdot V_{\mathrm{t}} \quad (3)$$

The Equation 1 suggests that possibly decrease of the powder mass would give rise to smaller $Q_{\max}$ i.e., the maximum quantity of trapped material in collision and hence possibly a higher rate of injected energy. The injection of higher energy transferred per unit quantity of material trapped in the collision event would also possibly give rise to a higher local temperature rise in collision event due to the higher rate of stress induced. The overall temperature of vial normally does not exceed 70°C, however, localized temperature rise at the point of collision might be involved. Since, the level of stress induced during mechanical activation is seen to be proportional to the temperature rise. Schwarz and Koch [28] have shown that the temperature rise, ΔT, induced due to the deformation in the powder can be expressed by:

$$\Delta T = kV'(2\tau/\pi\lambda C_{\mathrm{P}}\rho_{\mathrm{C}})^{0.5}, \quad (4)$$

where, V' is the shock velocity, k stress, λ, C_{P}, and ρ_{C} are the thermal conductivity, the heat capacity and the density of the deforming species, respectively, and τ is the stress state life time [29] expressed by:

$$\tau = V^{-0.2}(\rho_{\mathrm{b}}/E_{\mathrm{b}})^{0.4} R, \quad (5)$$

where ρ_{b}, is the density of ball, E_{b}, the elastic moduli of the ball and R the ball radius. Of course, it should be added that, for a given condition, the rate of the temperature rise is influenced by the change of particle size in nanometer size range. Since, one should consider the possible change of heat capacity and thermal conductivity with particle size in nanometer scale [30]. Based on the TEM work carried out in this work, nucleation of some nanocrystalline phases was observed in an amorphous phase. Nucleation of nanocrystalline lead scandium tantalite (PST) regions [31] and nanocrystalline complex perovskite phase PZN-PMN-PT [32] in amorphous matrices have also been reported to form during the early stage of mechanical activation by high resolution transmission electron microscope (HRTEM). Further, the growth of these nanocrystalline islands were seen to happen, converting the whole matrix into a nanocrystalline phase by applying appropriate activation conditions. Fig. 7 implies a simple one-dimensional schematic presentation of such arrangements of the atoms in a nanoscale particle, based on the reported results [31, 32] and the presented work here. The formation of single phase PZT compound for the sample prepared by planetary mill with a BPR = 20 at 500 rpm in this work is thought to be due to a higher injected energy and consequent higher temperature rise

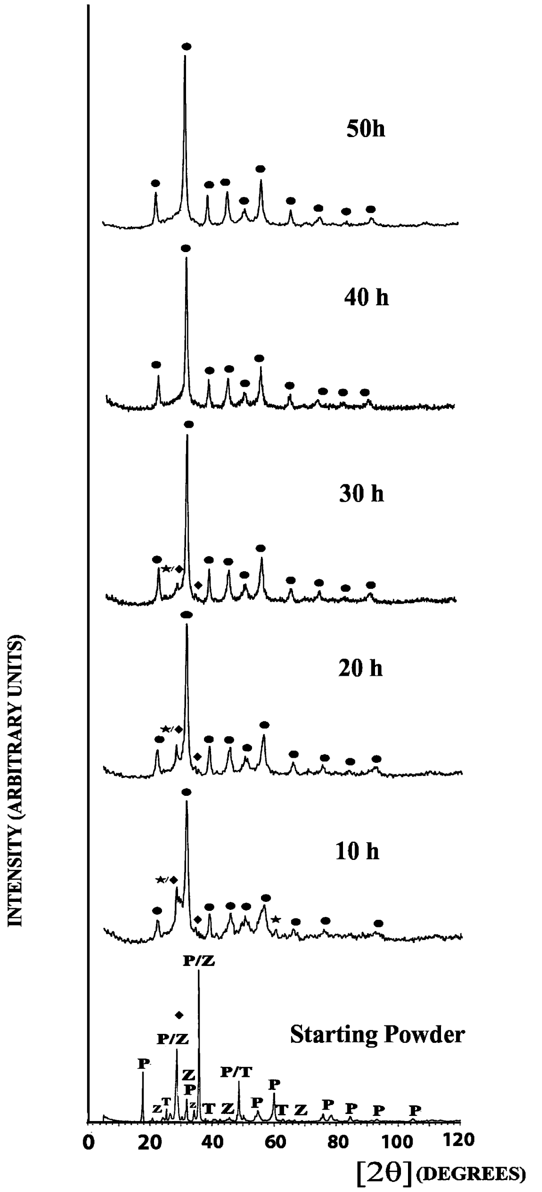

Figure 8 XRD multiplot of the PZT composition subjected to mechanical activation at various times using a shaker mill with BPR = 10 at 900 rpm. In this figure (P) stands for PbO, (Z) for ZrO_2, (T) for TiO_2, (*) $(PbO)_x$, (♦) $(ZrO_2)_x$, (●)PZT.

happened which would have possibly initiated a higher rate of grain boundary and lattice diffusion processes. This might have consequently caused the enhanced nuclei growth of nanocrystalline regions observed in an amorphous matrix reported in this work and shown by others. However, this has not possibly happened for the samples prepared by planetary mill with BPR = 10/1 and at 250 and 500 rpm where, possibly due to a lower grain boundary and lattice diffusion rate the formed nanocrystalline nuclei did not have the chance of further growth. Thus, One can therefore possibly anticipate a threshold level of impact energy and frequency required for the formation of single phase PZT.

Further, Fig. 8 displays XRD multiplot of the picked up samples at various time intervals e.g., 0, 10, 20, 30, 40 and 50 h with high energy shaker mill at 900 rpm and a BPR = 10/1. For these series of samples, here after just 10 h of milling, the sharp peaks of mixed oxides seen for the non-activated sample have vanished, suggesting a significant refinement in crystallite and particle sizes of the constituent oxides and possibly formation of some intermediate solid solutions. XRD results for these series of samples (Fig. 8) confirmed the onset of formation of PZT phase just after 10 h of milling and the formation of single phase PZT only after 30 h. This can be also justified based on the above discussion, that is, due to the injection of higher impact energy transferred to the mixed powder compared to other series of samples prepared in this work by planetary mill. The average crystallite size estimated from XRD data for the sample prepared by shaker mill for 40 h was ∼10 nm.

4. Conclusions

The below mentioned conclusions are obtained based on the work presented here:

1. The BPR and milling speed was seen to have a marked influence on the phase formation of PZT nanocrystalline powder prepared by planetary mill.
2. Single phase PZT nanocrystalline powder prepared by planetary mill could only be formed with a BPR = 20 and milling speed of 500 rpm after 65 h. The occurrence of a higher grain boundary and lattice diffusion rate possibly due to the higher local temperature rise in collision event is thought to explain the results.
3. For the samples prepared by shaker mill, the formation of single phase PZT was seen to take place in much shorter time compared to that of the samples prepared by planetary mill.

Acknowledgements

The authors would like to thank Iran University of Science and Technology (IUST) for the support of the work. Further, we would like to acknowledge the kind help Prof. W. Oesterle from BAM Federal Institute for Material Research and Testing, Berlin Germany for TEM studies.

References

1. H. GLEITER, *Nanostruct. Mater.* **1** (1992) 1.
2. R. BIRRINGER, *Mater. Sci. Eng.* A **117** (1989) 33.
3. C. SURYANARAYANA, *Int. Mater. Rev.* **40** (1995) 41.
4. I. Z. JIANG, R. LIN, W. LIN, K. NIELSEN, S. MORUP, K. DAM-JOHANSEN and R. CLASEN, *J. Phys. D: Appl. Phys.* **30** (1997) 1458.
5. J. Z. JIANG, F. W. POULSEN and S. MORUP, *J. Mater. Res.* **14** (1999) 1343.
6. D. J. FATEMI, V. G. HARRIS, V. M. BRONING and J. P. KIRKLAND, *J. Appl. Phys.* **83** (1998) 6767.
7. X. JUNMIN, T. YUNLING, W. DONGMEI and J. WANG, *Solid State Ionics* **120** (1999) 183.
8. C. GOMEZ-YANES, C. BENITEZ and H. BALMORI-RAMIREZ, *Ceram. International* **26** (2000) 271.
9. X. JUNMIN, J. WANG and T. WEISENG, *J. Alloys Compd.* **308** (2000) 139.
10. L. B. KONG, W. ZHU and O. K. TAN, *J. Mater. Sci. Lett.* **19** (2000) 1963.
11. A. J. MOULSON and J. M. HERBERT, in "Electroceramics, Materials, Properties and Applications" (Chapman and Hall, London, 1990) p. 277.
12. T. R. N. KUTTY and R. BALACHANDAN, *Mater. Res. Bull.* **19** (1984) 1479.
13. K. R. M. RAO, A. V. P. ROS and S. KOMARNENI, *Mater. Lett.* **28** (1996) 463.
14. H. HIRASHIMA, E. ONISHI and M. NAKAGOWA, *J. Non-Cryst. Solids* **121** (1990) 404.
15. X. JUNMIN, W. DONGMEI, S-E. LEE and J. WANG, *J. Amer. Ceram. Soc.* **82** (1999) 1687.
16. S. BEGIN-COLIN, G. LE CAER, M. ZANDONA, E. BOUZY and B. MALAMAN, *J. Alloys Compd.* **227** (1995) 157.
17. E. GAFFET, M. ABDELLAOUI and N. MALHOUROUX-GAFFET, *Mater. Trans. JIM* **36** (1995) 198.
18. EL-ESKANDARANI and M. SHERIF, in "Mechanical Alloying for Fabrication of Advanced Engineering Materials" (Norwich, New York, Noyes, Pub., 2001) p. 14.
19. L. B. KONG, W. ZHU and O. K. TAN, *Mater. Lett.* **42** (2000) 232.
20. B. D. CULLITY, in "Elements of X-ray Diffraction" (Addison Wesley, Pub. Co. Inc., 1978) p. 284.
21. G. B. SCHAFFER and P. G. MCCORMIK, Mechanical *Alloying, Mater. Forum* **16** (1992) 91.
22. P. G. MCCORMIC, V. N. WHARTON, M. M. ROYHAIR and G. B. SCHAFFER, in "Microcomposites and Nanophase Materials" (TMS Warrendale, Pennsylvania, 1991) p. 65.
23. L. LU, M. O. LAI and S. ZHANG, *Mater. Week* **94** (1994) 522.
24. H. V. ATKINSON and B. A. RIKINSON, in "The Adam Hilger Series on New Manufacturing Processes and Materials," edited by J. Wood (Adam Hilger, Bristol, Philadelphia and New York, 1991) p. 34.
25. M. ABDELLAOUI and E. GAFFET, *J. Alloys Compd.* **209** (1994) 351.
26. *Idem., Acta Metall. Mater.* **43** (1995) 1087.
27. M. MAGINI and A. IASONNA, *Mater. Trans. JIM* **36** (1995) 123.
28. R. B. SCHWARZ and C. C. KOCH, *Appl. Phys. Lett.* **49** (1986) 146.
29. D. R. MAURICE and T. H. COURTNEY, *ibid.* **21A** (1990) 289.
30. H.-J. FECHET, *Nanostruct. Mater.* **6** (1995) 33.
31. J. LIM, X. JUNMIN and J. WANG, *Scripta Mater.* **44** (2001) 1803.
32. D. M. WAN, J. M. XUE and J. WANG, *Mater. Sci. Eng.* A **286** (2000) 96.

Received 11 September 2003
and accepted 27 February 2004